1

Advances for Tsunami Measurement Technologies and Its Applications

Hiroyuki Matsumoto
Japan Agency for Marine-Earth Science and Technology, Japan

1. Introduction

After the Indian Ocean tsunami from the Sumatra earthquake on 26 December 2004 (Mw > 9.0), we have realized the importance of the early tsunami warning system and its necessity for mitigating the tsunami disaster. This catastrophic event was a cue for construction of the Indian Ocean early tsunami warning system, and first of all, a global tsunami forecast system was established together with the Pacific Ocean tsunami warning system operated by U.S. and Japan. The Indian Ocean tsunami motivated the international scieity to construct global tsunami warning systems, which include seismic and sea level monitoring measurements. National Centre of Geosciences in Germany, for example, would challenge to detect relative initial tsunami height distribution by GPS arrays and the seismic stations on land, and deploy GPS buoys along the Sumatra trench for establishment of an early tsunami warning system in Indonesia. And finally the German-Indonesian Tsunami Early Warning System (GITEWS) become into operation in 2010 (e.g., Rudloff et al., 2009; Münch et al., 2011).

Before the Indian Ocean tsunami in 2004, only tide gauge records are available data in the most countries surrounding the Indian Ocean (e.g., Merrifield et al., 2005; Matsumoto et al., 2009). Moreover, some of them were not transfered in real-time but were recorded and avaliable only inside the tide gauge stations. Instrumentally observed tsunami data acquired in real-time is qualitatively used for tsunami warning issue followed by its modification and cancellation. If characteristics of forthcoming tsunami would be understood in advance, it must be helpful and useful for tsunami related disaster mitigation. Tsunami height and arrival time are the most important information after the tsunamigenic earthquake occurrence, and they are often used as tsunami observation information. Tsunami observation is traditionally carried out by tide gauges at the coast. Recently, technological development has been promoted to estimate tsunami features as early as possible.

This chapter reviews tsunami measurement technologies and instruments, in particularly developed in Japan and introduces an actual tsunami observation in the source area, which became possible after the offshore tsunami observation in the last decade. In the end, potential use for early tsunami detection is discussed by applying to the presumed megathrust earthquake in the Nankai trough, SW Japan.

2. Tsunami measurement instruments

Tsunami measurements are usually carried out by tide gauge or bottom pressure sensor, or kinematic GPS buoy in Japan. The most traditional procedure is to measure by tide

gauge, whereas the most modern is by kinematic GPS buoy actually being in operation. Distribution of tsunami measurement instruments in Japan is shown in Fig. 1. This section describes details of tide gauge, bottom pressure sensor, and kinematic GPS buoy in their basic mechanism, outstanding problems, and applications of actual tsunami observation.

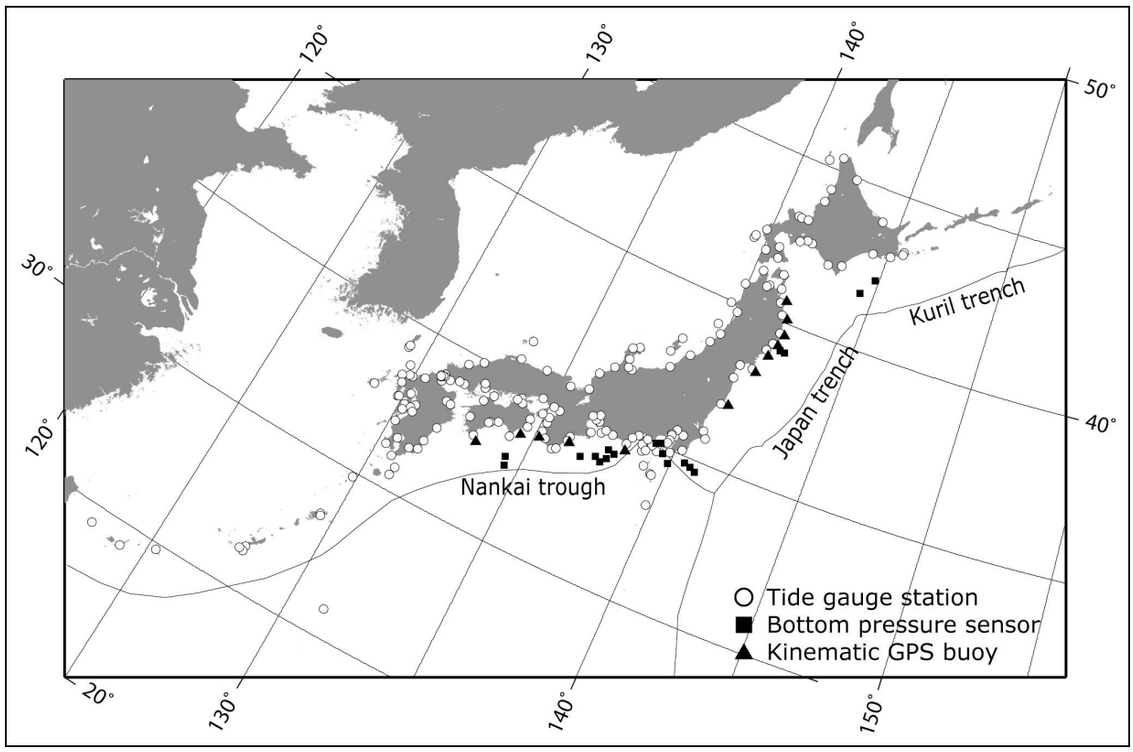

Fig. 1. Locations of tide gauge stations (open circles) and offshore tsunami observatories (kinematic GPS buoys: triangles; bottom pressure sensors: squares) in Japan.

2.1 Tide gauge

Tide gauges are deployed in order for measurement of usual sea level, i.e., astronomical tide level not only in Japan but also all over the world. Several types of tide gauges are being operated in Japan. The most typical tide gauge is to use a tide well which records vertical motion of a float buoy in a well connecting by an intake pipe to the open sea (Fig. 2). The first tide gauge was established in Japan is the in the early 1890s, for which Kelvin type tide gauge produced in England was employed (GSI, available at online). This type of tide gauge had used the analogue paper chart until the 1990s, and more recently digital decoding instrument is equipped on the tide gauge. The tide gauge using a paper chart requires replacement of recording paper at some intervals. Other types of tide gauges are as follows, e.g., a pressure type which measure hydrostatic pressure equivalent to the sea level at the station, and an acoustic type which measure distance between the sea surface and the acoustic receiver at the bottom. Generally, tide gauge stations are located inside the port or the harbour. This is why tsunami height based on tide gauge means tendency value where the tide gauge station is located. In fact, tsunami heights vary depending on both the local land and subsea topographies.

Another concern to make use of tide gauge is its response. Differences on tsunami heights between tide gauges and eyewitnesses have been pointed out in the past. Tide gauge generally uses a narrow intake pipe between the tide well and the sea as shown in Fig. 2. This is because the main purpose of tide gauge is to observe astronomical tide with its period of a few hours or much longer of a few years' sea level change caused by global climate change. Hence short period sea level changes such as surge wave or swell are structurally cut off. Tsunamis of their period less than a few ten of minutes can be recorded by tide gauges indeed, but some considerable responses were pointed out in the past. For example Okada (1985) examined the tide gauge response after the Japan Sea earthquake (Mw7.9) in 1983, and corrected tsunami waveform in terms of nonlinear response. Namegaya et al. (2009) carried out in-situ measurement of tide gauge stations and estimated liniear and nonlinear response and corrected the tsunami waveforms from the Niigataken Chuetsu-oki, Japan eartqhauke (Mw6.6) in 2007.

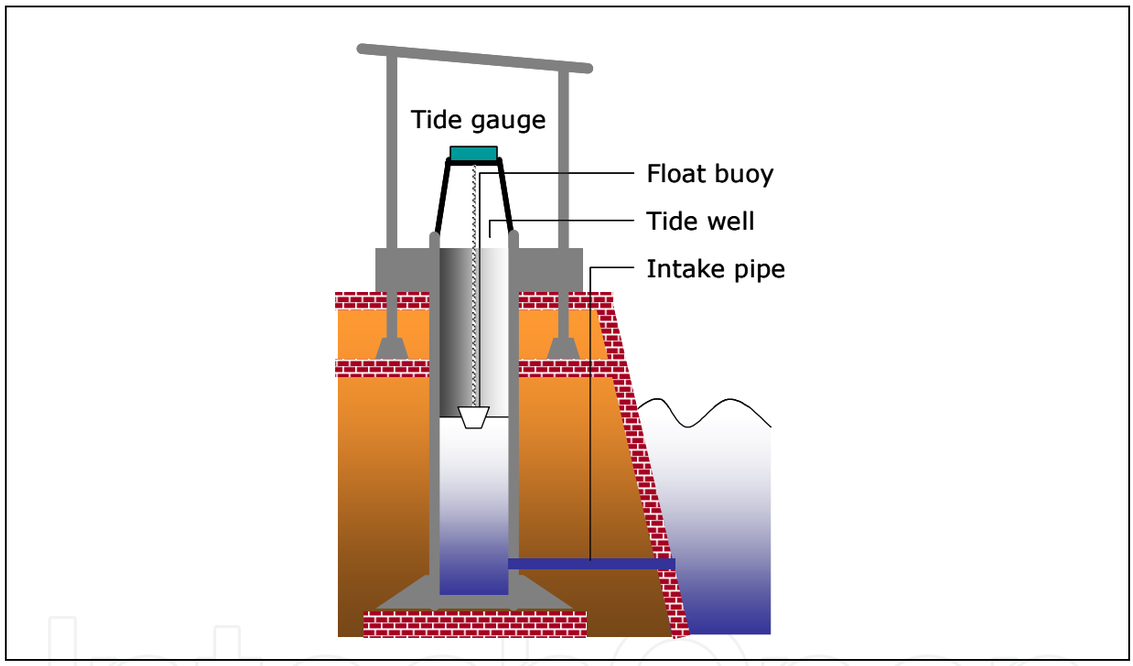

Fig. 2. Schematic drawing of typical float type tide gauge station in Japan.

2.2 Bottom pressure sensor

Offshore tsunami measurement makes us possible to predict tsunami arrival and provide time to evacuate from tsunami. Recent deep-sea technologies enable to observe tsunamis not only offshore but also in real-time. One of the facilities composing the early tsunami warning system is the offshore observatory. National Oceanic and Atmospheric Administration (NOAA) developed Deep-ocean Assessment and Reporting of Tsunamis (DART) system that receives water pressure from the ocean bottom firstly deployed in the Pacific and Atlantic Oceans (Gonzalez et al., 2005). Now the DART system has been extended to the Indian Ocean and each observatory is owned by not only U.S. but also Australia, Chile, Indonesia Thailand, and Russia. On the other hand, other sensors such as in-lined cabled bottom pressure sensors are developed and deployed in the seismogenic

zone in Japan. Figure 1 represents the current bottom pressure sensors locations being operated in Japan either. The first offshore observatory in Japan has been deployed in 1978 off Omaezaki, central Japan, where the probability of the presumed Tokai earthquake is expected to be 87 % by the Earthquake Research Committee of the Headquarters for Earthquake Research Promotion, i.e., the Japanese Government. Then this types of tsunami measurement have followed until now, and eight observatories in total have been deployed in Japan.

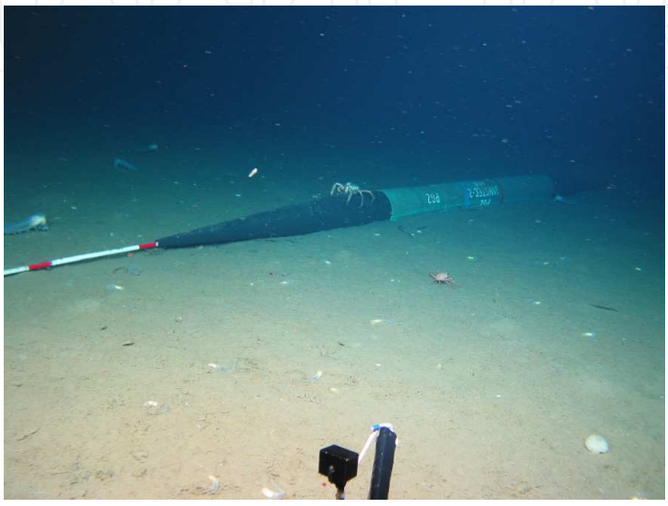

Fig. 3. In-lined cabled bottom pressure sensor deployed in the ocean.

Offshore tsunami detected by bottom pressure sensor is given by Filloux (1982) for the first time. Eble and Gonzalez (1986) performed the long-term observation on bottom pressure sensors and reported detection of offshore tsunami signals from three different earthquakes during their observational period. Hino et al. (2001) and Hirata et al. (2003), for example, used less than a few centimetres tsunamis from the moderate-to-large earthquakes occurred in the Japan trench and the Kuril trench, respectively, that could be detected by Japanese cabled bottom tsunami sensors. Matsumoto and Mikada (2005) and Satake et al. (2005) used offshore tsunami recorded by bottom pressure sensors in order to constrain fault models of the off Kii peninsula earthquake (Mw 7.4) in Japan, and demonstrated advances offshore observation for tsunami. Tsunami from the off Kii peninsula earthquake was also observed at the tide gauge stations along the coast nearby. Bottom pressure sensors could detect tsunami signals about 20 min before its arrival at the nearest tide gauge stations. Thus it shows that offshore tsunami observation has an advantage of the tsunami detection for far-field tsunamis.

2.3 Kinematic GPS buoy

Kinematic GPS buoy is a new technological system developed in the late 1990s to observe tsunami at the offshore sea surface (Kato et al., 2000). GPS, i.e. Global Positioning System technology widely used on land is to be applied to the sea surface. The current kinematic GPS buoy monitors a moving platform in real-time with an accuracy of a few centimetres by relative positioning. It requires two GPS receivers to measure the relative position, one is

placed on the top of offshore buoy and the other is placed on land-based station. After practical operation period, about 10 kinematic GPS buoys have been deployed 10-20 km offshore from the coast in Japan (Figs. 1 and 4). Although GPS buoy cannot be deployed over several kilometres further offshore because of the limitation of communication distance between the GPS buoy and the base station, it has demonstrated an advantage for early tsunami detection. The tsunami from the off Kii peninsula earthquake was recorded by the GPS buoy for the first time 8 min before its arrival at the nearest tide gauge station (Kato et al., 2005). Tsunami from the off Kii peninsula earthquake was detected by both the offshore pressure sensors and the kinematic GPS buoys in which tsunami heights were recorded to be ca. 10 cm and ca. 20 cm in peak-to-peak amplitude, respectively, whereas the tsunami height recorded by the tide gauge was to be 50 to 100 cm. This is attributed to the shoreing effect.

Fig. 4. Kinematic GPS buoy deployed offshore of NE Japan (photo by Port and Airport Research Institute).

3. Tsunami measurement applications

Offshore tsunami observation has an advantage for far-field tsunami as mentioned above. However, for the near-field tsunamis that are generated near the tsunami measurement sensors it have not been experienced and discussed about usage of acquired data. This section describes an example of actual tsunami observations in particular in the near-source area by the bottom pressure sensors by the cabled observatory system, and discuss their unique phenomena during the tsunami generation process for use of tsunami early detections. Offshore tsunami observations have been done in the past as reviewed in the previous section. At the beginning of the offshore observation of tsunami, pressure fluctuation caused by the seismic wave apparently much intense than that by the tsunami wave (e.g., Filloux, 1982). This is why mathematical low-pass filtering is necessary to detect tsunami signals. In fact, low-pass filtering was applied in most cases of tsunamigenic earthquakes in order to identify tsunami signals afterwards for scientific

purpose. In Japan, the Japan Meteorological Agency (JMA) is responsible for tsunami warning issue, and offshore measurement data are processed by using 1-2 min moving averaging technique. If a large earthquake would take place offshore and accompany a tsunami, i.e., a far-field tsunami, it would not be so difficult to notify tsunami signals as done by the present procedure. Most pressure sensors have been deployed in the tsunami source area. For near-field tsunami, however, there has not been established that data processing methods prepared so far. We urgently need data processing procedure for the near-field tsunamis.

3.1 Bottom pressure sensor off Hokkaido, Japan

Japan Agency for Marine-Earth Science and Technology (JAMSTEC) is operating four offshore observatories in the seismogenic zone in Japan; off Muroto cape and off Kumano in the Nankai trough, SW Japan, off Hatsushima Island in the Sagami trough, central Japan, and off Hokkaido in the Kuril trench, northern Japan. The present study introduces the offshore observatory off Hokkaido deployed in 1999 (Hirata et al., 2002). Figure 5 shows that the location of bottom pressure sensors connecting by the submarine cable. The cabled observatory has two bottom pressure sensors, and those data is telemetered to JAMSTEC in real-time. Two bottom pressure sensors as referred by PG1 and PG2 hereafter are deployed at the water depths of 2218 m and 2210 m, respectively, and their locations are listed in Table 1.

A megathrust M8.0 earthquake occurred in 2003 in this region (Watanabe et al., 2004), and then the seismic activities including aftershocks have become relatively high. A number of earthquakes over their magnitude 6.0 took place after 2003. In the present study, we focus on the near-field earthquakes in order to understand the observed fluctuation of water pressure during the tsunamigenic earthquake. Referring the earthquake database complied by JMA, earthquakes occurred inside ca. 100 km from the observatories are selected. Because a bottom pressure sensor is very sensitive, we focus on large earthquakes with their

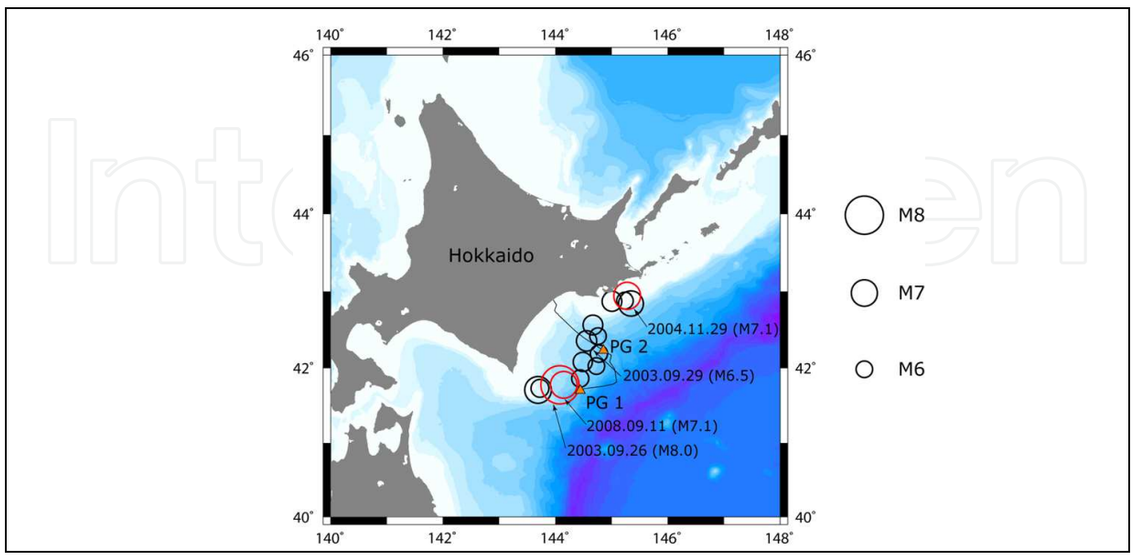

Fig. 5. Offshore observatory off Hokkaido, Japan with locations of significant earthquakes' epicenters. Red indicates a tsunamigenic earthquake.

magnitude over 6.0 by means of signal-to-noise ratio. Conditioning these criteria, 16 earthquakes were selected listed in Table 2. Among those 16 earthquakes, three earthquakes on 26 September 2003, on 29 November 2004, and 11 September 2009 generated the tsunamis which were observed at the tide gauge stations at the coast. Locations of the selected earthquakes and the PGs are compared in Figure 5. Both the 2003 and 2009 tsunamigenic earthquakes' epicenters were located beneath PG1, on the other hand, that of the 2004 earthquake was located out of PGs.

	Latitude (◦N)	Longitude (◦E)	Water depth (m)
PG1	41.7040	144.4375	2218
PG2	42.2365	144.8454	2210

Table 1. Location of bottom pressure sensors off Hokkaido, Japan.

	Date	Time (JST)	Latitude (◦N)	Longitude (◦E)	Depth (km)	Magnitude	Tsunami
1	2003.09.26	04:05:07.42	41.779	144.079	45.1	8.0	observed
2	2003.09.26	06:08:01.84	41.710	143.692	21.4	7.1	
3	2003.09.26	15:26:58.10	42.189	144.776	27.4	6.1	
4	2003.09.27	05:38:22.31	42.026	144.728	34.4	6.0	
5	2003.09.29	11:36:55.06	42.360	144.553	42.5	6.5	
6	2003.10.08	18:06:56.79	42.565	144.670	51.4	6.4	
7	2003.10.11	09:08:48.15	41.864	144.440	27.8	6.1	
8	2003.12.29	10:30:55.40	42.419	144.756	38.9	6.0	
9	2004.11.11	19:02:46.17	42.083	144.486	38.6	6.3	
10	2004.11.29	03:32:14.53	42.946	145.276	48.2	7.1	observed
11	2004.11.29	03:36:41.19	42.884	145.236	45.6	6.0	
12	2004.12.06	23:15:11.81	42.848	145.343	48.8	6.9	
13	2005.01.18	23:09:06.65	42.876	145.007	49.8	6.4	
14	2007.02.17	09:02:56.63	41.732	143.723	40.1	6.2	
15	2008.09.11	09:20:51.35	41.776	144.151	30.9	7.1	observed
16	2009.06.05	12:30:33.80	41.812	143.620	31.3	6.4	

Table 2. Significant earthquakes occurred near the pressure sensors off Hokkaido, Japan.

3.2 Data processing procedure

Generally, bottom pressure sensors measure the vibration regarding pressure and temperature, from which physical value is processed compensating the temperature collections. For the principal of the pressure sensors, narrow sample rate gives low resolution response. 10 Hz sampling is the minimum sample rate for the reliable value. We have analyzed the obtained PGs dataset to make spectrograms. Numerical technique to analyze 10 Hz time-series PGs dataset is as follows;

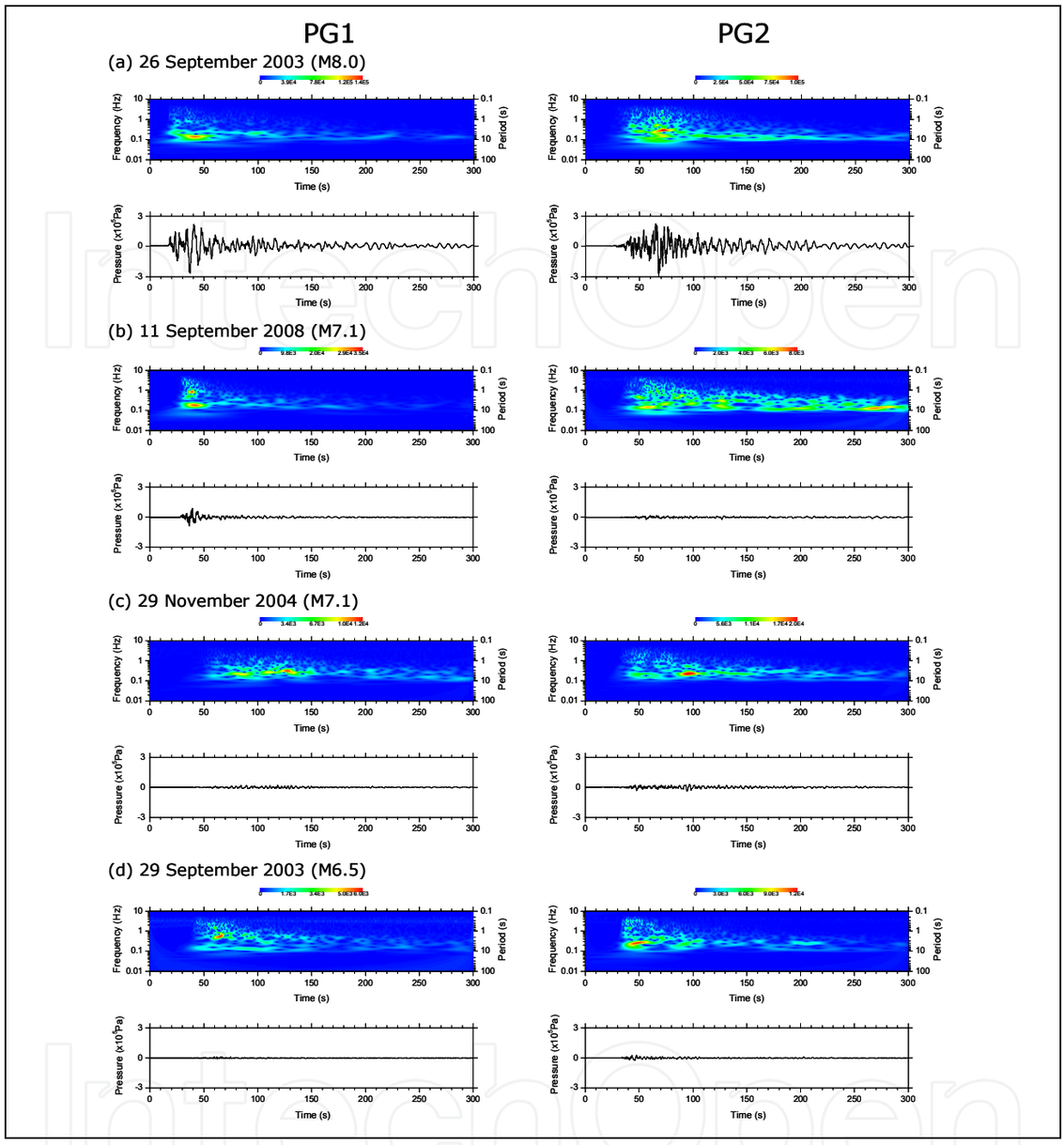

Fig. 6. Pressure waveforms' spectrograms and its original waveforms during the earthquakes.

1. 5min dataset of PG including each earthquake is collected.
2. We divide the frequency from 0.01 Hz to 10 Hz into 40 sections as formed by exponentially (i.e., linearly in logarithmic scale).
3. Band-pass filtering of each section above is applied to the entire 5min dataset.
4. Envelopes of the filtered waveforms for each section are layout to get absolute amplitude, and spectrogram of PGs during the earthquake can be made.

Spectrograms with the original pressure waveforms during the tsunamigenic earthquakes on (a) 26 September 2003 (M8.0), (b) 11 September 2008(M7.1), and (c) 29 November 2004 (M7.1) are plotted in Fig. 6, and the largest non-tsunamigenic earthquake on (d) 29 September 2003

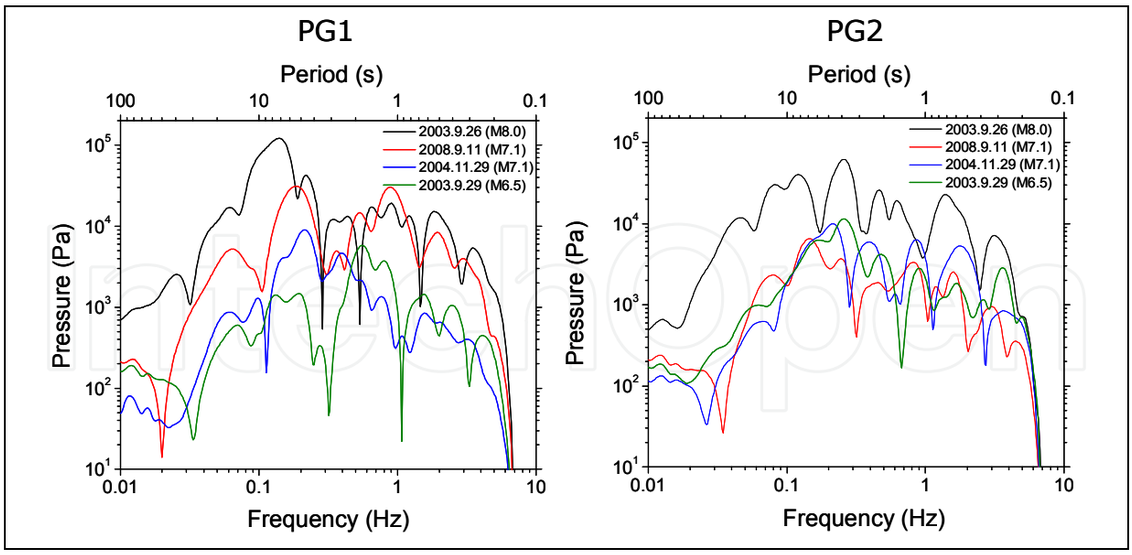

Fig. 7. Cross section profiles of spectrograms during the earthquakes.

(M6.5) is also displayed as an example. According to the spectrograms in the near-field, i.e., event (a) and (b), strong phase having 0.1 to 0.2 Hz is obviously observed during the tsunamigenic earthquake. Tsunamigenic earthquake out of the PGs, i.e., event (c), their characteristic phase appeared after the earthquake rather than during the earthquake. This is because this phase is reproduced in the tsunami source area, and then it propagates.

Cross section profiles of the spectrogram during the earthquakes are plotted in Fig. 7. Tsuamigenic events have peak from 0.1 to 0.2 Hz, which correspond to a natural frequency uniquely depending on the water depth. This is an acoustic resonant wave, i.e., a standing wave forming between the ocean bottom and the sea surface caused by the coseismic deformation (e.g., Nosov & Kolesov (2007)). The larger earthquake magnitude becomes, the larger water pressure amplitude responses in its narrow band.

Thus the tsunamigenic earthquake has a peak of frequency between 0.1 Hz and 0.2 Hz in the case of the water depth about 2000 m. And its peak attenuates in duration of 20 s. The same peak of frequency between 0.1 Hz and 0.2 Hz is involved during the non-tsunamigenic earthquake, but its peak is lower than the high frequency peaks associated with seismic waves.

3.3 Implication of water pressure

Maximum water pressure Pmax in the case of abrupt bottom deformation resulting in tsunami generation process is expressed as multiplication of density of water ρ, sound velocity in water v, and the bottom deformation velocity v,

$$P_{max} = \rho\, c\, v \tag{1}$$

Because density and sound velocity are constant, i.e., 1.03 kg/m^3 and 1500 m/s, resptctively, Eq. (1) provide the bottom velocity. For example, (a) the 2003 and (b) the 2008 earthquake cases, the bottom deformation velocity are given to be 0.13 m/s and 0.03 m/s, respectively.

On the other hand, the empirical relation between earthquake magnitude M and rise-time of the seismic faulting τ is proposed by Sato (1979),

$$\tau = 10^{1.5M-1.4}/80 \quad (2)$$

Eq. (2) provides that the rise-times for (a) the 2003 and (b) the 2008 are 5.0 s and 1.7 s, respectively. Assuming the duration time of bottom deformation coincides with the rise-time of the seismic faulting, deformation is given by its velocity integrated by the rise-time. Thus derived deformations at the location of PG1 are estimated to be (a) 0.65 m and (b) 0.06 m, respectively. These values almost coincide with (a) the static deformation from the fault plate model by Geospatial Information Authority of Japan (GSI) (2003) and (b) the point source equivalent to the seismic moment (Fig. 8). This means that the displacement of the location of the pressure sensor deployment can be roughly estimated in terms of the water pressure amplitude.

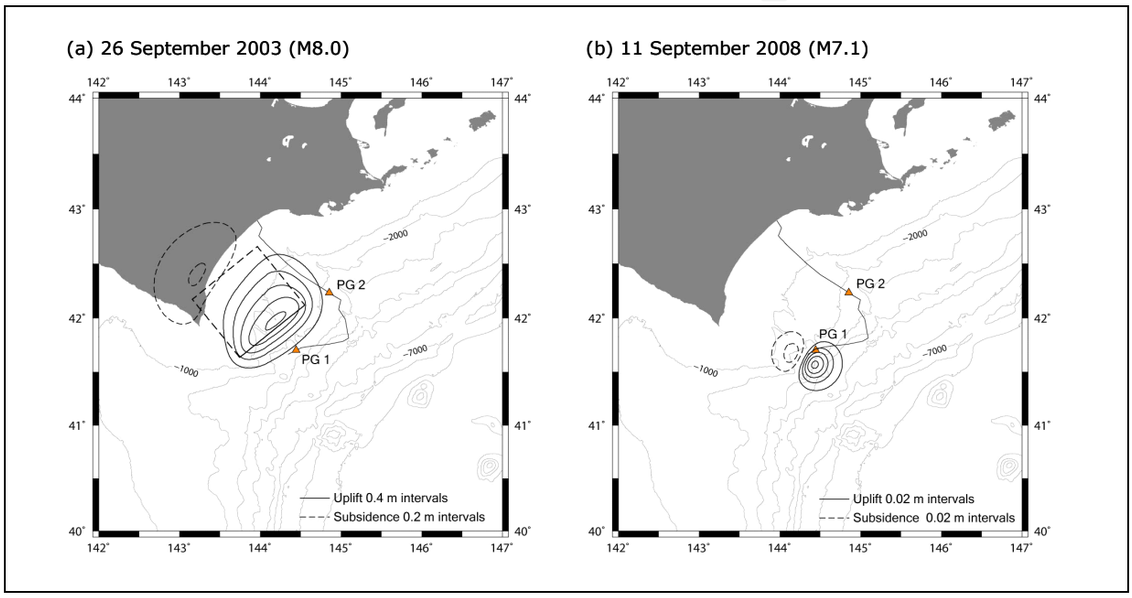

Fig. 8. Deformation patterns from the seismic faults' dislocation

An early tsunami detection approach based on a physical phenomenon uniquely observed in the source during the tsunamigenic earthquake was presented in this section. Tsunami initial waveform is mostly depended on the static deformation of the ocean bottom. Hence the amplitude of the water pressure associated with the acoustic resonant wave may be a potential indicator of the tsunami generation.

4. Tsunami prediction along the Nankai trough

The first offshore observatory in Japan has been deployed in the Suruga trough targetting the presumed Tokai earthquake, central Japan, and followed by seven cabled observatories. The newest system is being operated in the presumed Tonankai earthquake sourece area by JMA and JAMSTEC off Kii peninsula (Fig. 9).

4.1 Tsunami monitoring system in the Nankai trough

The Nankai trough is one of the palte subduction zones in Japan, where the last megathrust earthquakes took place in 1944 and 1946, namely the Tonankai eartqhauke and the Nankai

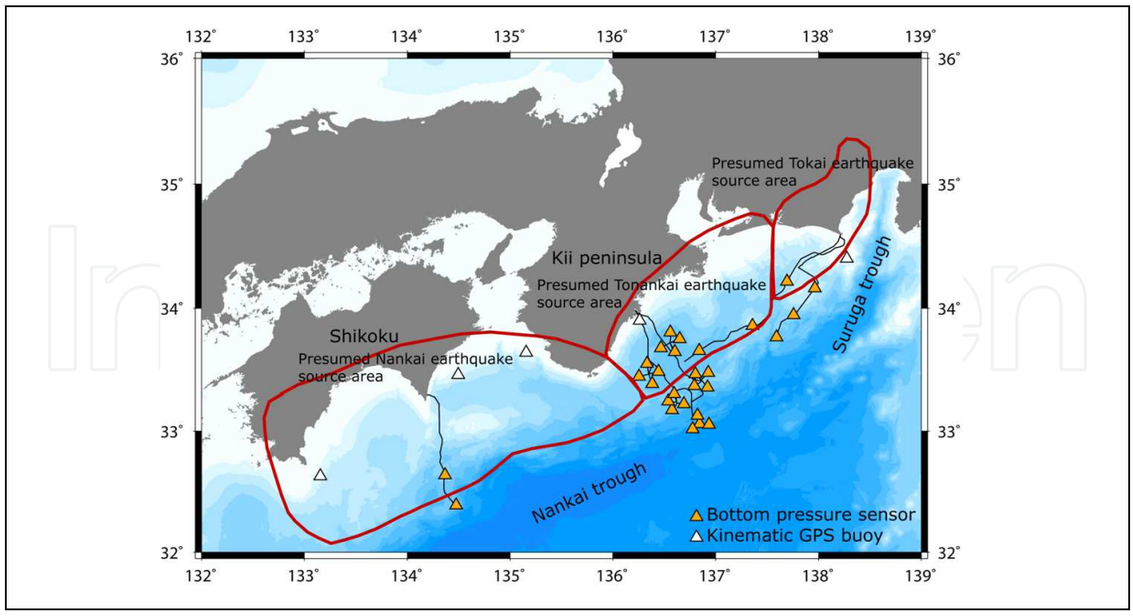

Fig. 9. Deformation patterns from the seismic faults' dislocation

earthquake, respectively. Because more than 60 years have past since the last earthquake, Japanese government evaluates that the probability of the next presumed megathrust earthquake along the Nankai trough is estimated to be 60-70 % within the next 30 years. Japanese government has constructed an offshore observatory network, which consists of dense 20 bottom seismic sensors and bottom pressure sensors in total in order for monitoring seismic activity and its consequence, megathrust earthquake, and followed by tsunami. JAMSTEC is operating the offshore observatory network. The observatory layout is shown in Fig. 10. As of May 2011, 17 observatories have been deployed, and it started to acquire their data in real-time. If megathrust earthquake and accompanied giant tsunami would be predicted before their arrival nearby the coast and effective warning would be issued, it must contribute to mitigate earthquake and tsunami related disasters. We should establish measurement technology including data processing and accumulate technical know-how for future meagathrust earthquake and tsunami in advance; hence we carry out tsunami computation of the last 1944 Tonankai earthquake.

Parameters	Value
Location	33.277 °N, 136.394 °E
Depth	10 km
Strike	226 °
Dip	10 °
Rake	90 °
Length	130 km
Width	60 km
Dislocation	2 m
Rise time	5 s
Rupture velocity	3 km/s

Table 3. Fault parameters used in the tsunami computation from the Tonankai earthquake.

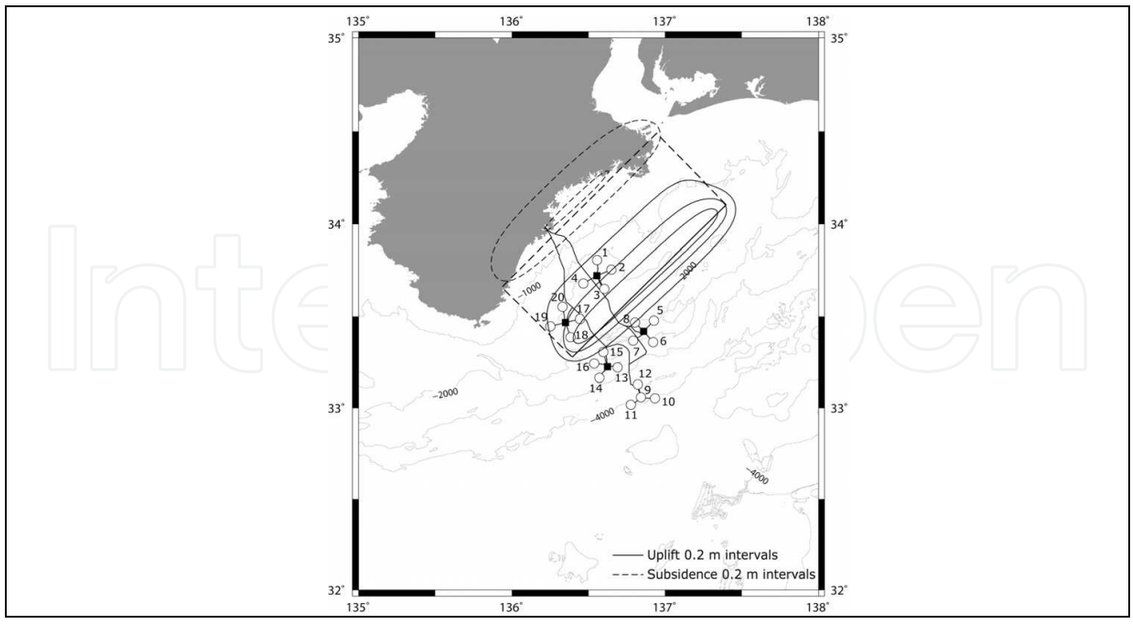

Fig. 10. Observaroty layout (open circles) and coseismic deformation caused by the seismic fault.

4.2 Tsunami computation from the presumed Tonankai earthquake

The latest study implies that the splay fault might contribute to the tsunami generataion process in addition to the main fault during the 1944 Tonankai earthquake (Park et al., 2002), however a simplified fault model is assumed and the pressure waveform is computed at the 20 observatories in the present study. Fault parameters are based on what has been estimated by Kanamori (1972) and they are listed in Table 3. Geometric relation between the fault plane and the observatories is shown in Fig. 10. It is assumed that the fault rupture starts from the bottom at the fault plane and propagate toward the top along the width direction, meaning uni-lateral faulting. Dynamic tsunami computation developed by Ohmachi et al. (2001) is applied to the present scenario. Dynamic tsunami computation can demonstrate fluid dynamic response due to the seismic fault rupture considering both the static deformation and the seismic wave in the tsunami computation. Dynamic tsunami computation can reproduce the bottom pressure because realistic 3D fluid domain is modeled.

Two different tsunami generation models are computed in the present study. One model is that the static deformation is given as a ramp-time function into the bottom of the fluid domain. The duration time, i.e., elapsed time to generate tsunami initial shape is assumed to be equal to the source time of the seismic faulting. Because the fault width and rupture velocity are assumed to be 60 km and 3 km/s, respectively, the time duration is solved to be 20 s divided by two parameters. In this model, the dynamic contribution of the ocean bottom is considered, but the seismic wave associated with the fault rupturing is not considered. Another model is that the seismic wave due to the fault rupturing is also considered, in which the ocean bottom is not displaced simultaneously in the tsunami source area. This model can demonstrate more realistic tsunami generation process than the former one.

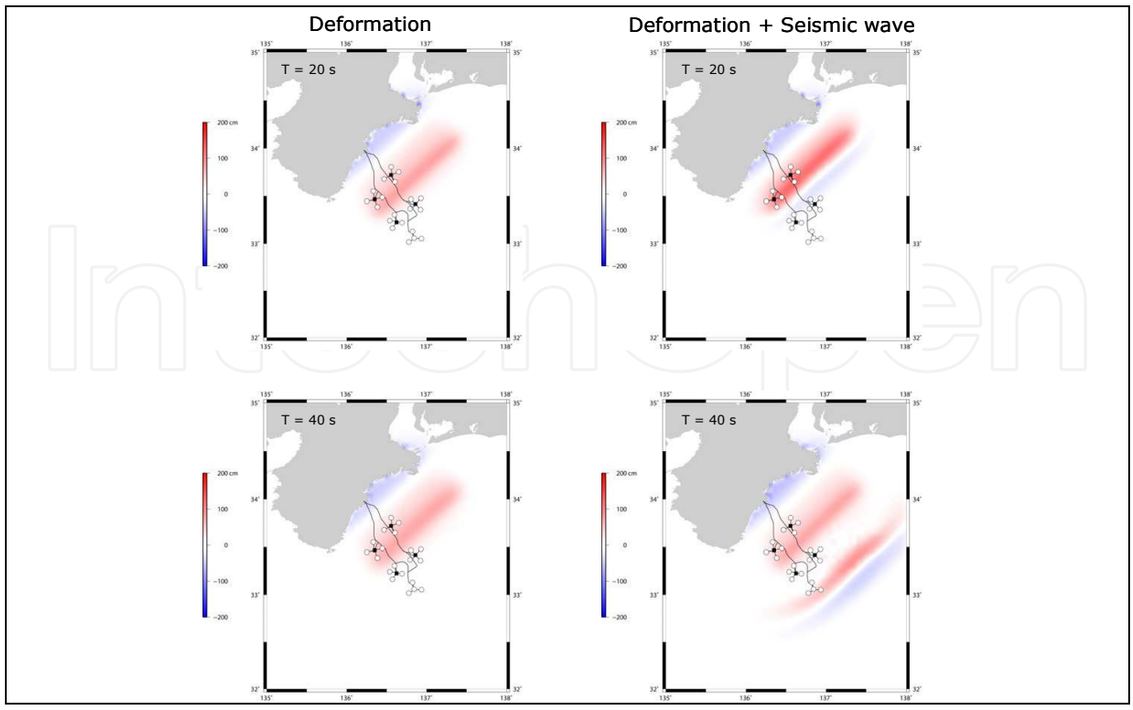

Fig. 11. Snapshots of wave height during the tsunami generation.

Snapshots of the tsunami generation are compared in Fig. 11. Although tsunami is generated after the fault rupture halt at 20 s in the both models, tsunami height in the source area is different. In the source area, dynamic effect is significantly appeared. This is because the acoustic wave by the seismic wave is superposed. At 40 s, the water wave propagating to SE direction is computed, which is Rayleigh wave. As for amplitude and source area of the tsunami are not so different each other.

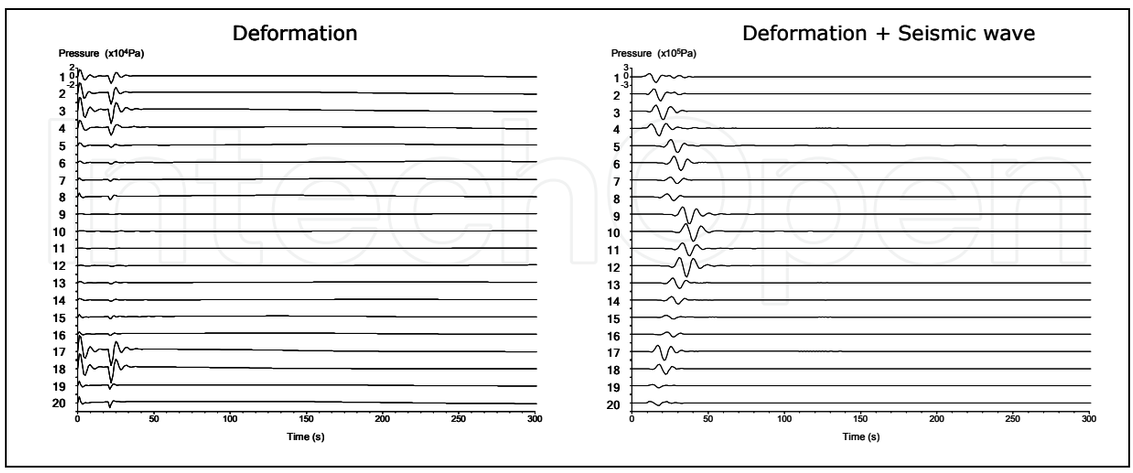

Fig. 12. Computed pressure waveforms during the tsunami generation at each observatory. Numberings represent that of the observatories in Fig. 10.

Time histories of water pressure at the observatories are shown in Fig. 12. In the case that only the bottom deformation is input, acoustic resonant wave is reproduced during the

tsunami generation. The amplitude corresponds to the distribution of the static deformation due to the seismic faulting. On the other hand, in the case that seismic wave is input to the fluid domain either, water pressure fluctuation associated with the Rayleigh wave is reproduced in addition to the water resonant wave. It should be noted that the maximum amplitude (~ a few of 10^5 Pa) is fairly equal to that of the experienced in the 2003 earthquake discussed in the previous section. The amplitude is obviously large at the offshore observatories such as 9, 10, 11, and 12 sites in the Nankai trough. These observatories are located in deeper area than others, hence the water pressures tend to be amplified by the long period Rayleigh wave. The acoustic resonant wave is an unique phenomenon during the tsunami generation process. Precise measurement of the acoustic resonant would provide tsunami generation prediction in advance.

5. Conclusion

This chapter reviews some tsunami measurements being in operation. Traditional tide gauge deployed at the coast is unable to perform early tsunami detection because of its deployed location. Recent offshore tsunami measurement technologies such as bottom pressure sensor and kinematic GPS buoy enabled to detect far-field tsunamis before its arrival at the coast. As an on-going study, HF radar to detect tsunami current approaching coast at long ranges is being developed and theoretically examined in the Atlantic Ocean (Dzvonkovskaya and Gurgel, 2009). More recently, electromagnetic (EM) sensors eventually could detect tsunami signals associated with its water mass passage from the 2006 and 2007 Kuil Is. earthquakes (Toh et al., 2011). Thus new tsunami measurement technologies and relevant sensors have been developed and applied for early tsunami detection in order for improving conventional tsunami warning system using bottom pressure sensors.

Then the present chapter introduces the actual observation of the bottom pressure sensors deployed in the tsunami source area. The acoustic resonant wave that is significantly produced in the tsunami generation process may contribute to the early tsunami detection scheme. Tsunami from the presumed Tonankai earthquake being though to take place within a next few decades is computed, which predict pressure waveforms at the offshore observatory in the source area. Acoustic resonant wave is computed in the tsunami source area, suggesting that its large amplitude implies large deformation. This gives an opportunity to issue an automated tsunami alert during the real-time monitoring by the bottom pressure sensors in the tsunami source area.

6. Acknowledgment

This study was partly supported by Grant-in-Aid for Young Scientist (B) 22710175 of the Ministry of Education, Culture, Sports, Science and Technology (MEXT), Japan. Some figures were prepared by Generic Mapping Tools (Wessel and Smith, 1995).

7. References

Dzvonkovskaya, A., & Gurgel, K. W. (2009). Future contribution of HF radar WERA to tsunami early warning systems, *European J. Navigation*, 7 (2), 17-23

Eble, M. C., & Gonzalez, F. I. (1991). Deep-Ocean bottom pressure measurements in the northeast Pacific, *J. Atom. Ocean. Tech.*, 8, 221-233

Filloux, J. H. (1982). Tsunami recorded on the open ocean floor, *Geophs. Res. Lett.*, 9, 25-28

Geospatial Information Authority of Japan. (online). History of Tide Gauges, available from http://tide.gsi.go.jp/ENGLISH/history.html

Geospatial Information Authority of Japan. (2003). Press release on 26 September 2003. available at http://www.gsi.go.jp/WNEW/PRESS-RELEASE/2003-0926-2.html

Gonzalez, F. I, Bernard, E. N., Meinig, C., Eble, M., Mofjeld, H. O. & Stalin S. (2005) The NTHMP tsunameter network, *Nat. Hazards*, 35, 25-39

Hino, R., Tnioka, Y., Kanazawa, T., Sakai, S, Nishino, M, & Suyehiro, K. (2001). Micro-tsunami from a local interplate earthquake detected by cabled offshore tsunami observation in northeastern Japan, *Geophys. Res. Lett.*, 28, 3533-3536

Hirata, K., Aoyagi, M., Mikada, H., Kawaguchi, K., Kaiho, Y., Iwase, R., Morita, S., Fujisawa, I., Sugioka, H., Mitsuzawa, K., Suyehiro, K., Kinoshita, H., & Fujiwara, N. (2002). Real-time geophysical measurements on the deep seafloor using submarine cable in the southern Kurile subduction zone, *IEEE J. Ocean. Eng*., 27, 170-181

Hirata K., Takahashi, H., Geist, E. L., Satake, K., Tanioka, Y., Sugioka, H., & Mikada, H. (2003). Source depth dependence of micro-tsunamis recorded with ocean-bottom pressure gauges: the January 28, 2000 Mw 6.8 earthquake off Nemuro Peninsula, Japan, *Earth Planet. Sci. Lett.*, 208, 305-318

Kanamori, H. (1972). Tectonic implication of the 1944 Tonankai and the 1946 Nankaido earthquakes, *Phys. Earth Planet. Inter.*, 5, 129-139

Kato, T., Terada, Y., Kinosita, M., Kakimoto, H., Issiki, H., Matsuishi, M., Yokoyama, A., & Tanno, T. (2000). Real-time observation of tsunami by RTK-GPS, *Earth Planets Space*, 52, 841-845

Kato, T., Terada, Y, Ito, K., Hattori, R., Abe, T., Miyake, T., Koshimura, S., & Nagai, T. (2005). Tsunami due to the 2004 September 5th off the Kii peninsula earthquake, Japan, recorded by a new GPS buoy, *Earth Planets Space*, 57, 297-301

Münch, U., Rudoloff, A. & Lauterjung, J. (2011). The GITEWS Project – results, summary and outlook, *Nat. Hazards Earth Syst. Sci.*, 11, 765-769

Matsumoto, H., & Mikada, H. (2005). Fault geometry of the 2004 off the Kii peninsula earthquake inferred from offshore pressure waveforms, *Earth Planets Space*, 57, 161-166

Matsumoto, H., Tanioka, Y., Nishimura, Y., Tsuji, Y., Namegaya, Y., Nakasu, T., & Iwasaki, S. (2009). Review of tide gauge records in the Indian Ocean, *J. Earthquake Tsunami*, 3, 1-15

Merrifield, M. A., Firing, Y. L., Aarup, T., Agricole, W., Brundrit, G., Chang-Seng, D., Farre, R., Kilonsky, B., Knight, W, Kong, L., Magori, C., Manurung, P., McCreery C., Mitchell, W., Pillay, S., Schindele, F., Shillington, F., Testut, L., Wijeratne, E. M. S., Galdwell, P., Jardin, J., Nakahara S., Porter F. Y., & Tuetsky, N. (2005). Tide gauge observations of the Indian Ocean tsunami, December 26, 2004, *Geophys. Res. Lett.*, 32, L09603, doi:10.1029/2005GL022610

Namaegaya, Y., Tanioka, Y., Abe, K., Satake, K., Hirata, K., Okada, M. & Gusman, A., R. (2009). In situ Measurements of Tide Gauge Response and Corrections of Tsunami Waveforms from the Niigataken Chuetsu-oki Earthquake in 2007, *Pure Appl. Geophys.*, 166, 97-116

Nosov, M. A., & Kolesov, S. V. (2007). Elastic ocsillations of water column in the 2003 Tokachi-oki tsunami sourece : in-situ measument and 3-D numerical modeling, *Nat. Hazards Earth Syst. Sci.*, 7, 243-249

Ohmachi, T., Tsukiyama, H., & Matsumoto, H. (2001). Simulation of tsunami induced by dynamic displacement of seabed due to seismic faulting, *Bull. Seism. Soc. Am.*, 91, 1898-1909

Okada, M. (1985). Response of some tide-wells in Japan to tsunamis, Proc. Int. Tsunami Symp., 208-213

Park, J. O., Tsuru, T., Kodaira, S., Cummins, P. R., & Kaneda, Y. (2002). Splay fault branching along the Nankai subduction zone, *Science*, 297, 1157-1160

Rudloff, A, Lauterjung, J. Münch, U. & Tinti, S. (2009). The GITEWS Project (German-Indonesian Tsunami Early Warning System), *Nat. Hazards Earth Syst. Sci.*, 9, 1381-1882

Satake, K., Baba, T., Hirata, K., Iwasaki, S., Kato, T., Koshimura, S., Takenaka, J., & Terada, Y. (2005). Tsunami source of the 2004 off the Kii Peninsura earthquakes inferred from offshore tsunami oand coastal tide gages, *Earth Planets Space*, 57, 173-178

Sato, R. (1979). Theoretical baseis on relationship between focal parameters and earthquak magnitude, *J. Phys. Earth*, 27, 353-372

Toh, H., Satake, K., Hmano, Y., Fujii, Y. & Goto, T. (2011). Tsunami signals from the 2006 and 2007 Kuril earthquakes detected at a seafloor geomagnetic observatory, *J. Geophs. Res.*, 116, B02104, doi:10.1029/2010JB007873

Watanabe, T., Matsumoto, H., Sugioka, H., Mikada, H., Suyehiro, K., & Otsuka, R. (2004) Offshore monitoring system records recent earthquake off Japan's northernmost island, *EOS Trans. AGU*, 85, 14

Wessel, P. & Smith W. H. F. (1995). New version of the Generic Mapping Tools released, *EOS Trans. AGU*, 76, 329.

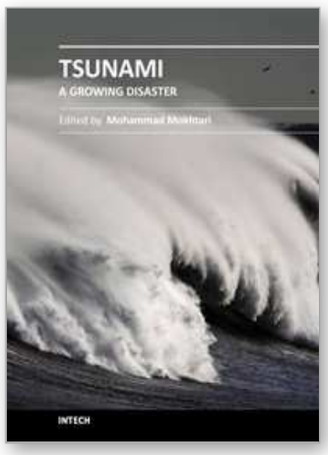

Tsunami - A Growing Disaster
Edited by Prof. Mohammad Mokhtari

ISBN 978-953-307-431-3
Hard cover, 232 pages
Publisher InTech
Published online 16, December, 2011
Published in print edition December, 2011

The objective of this multi-disciplinary book is to provide a collection of expert writing on different aspects of pre- and post- tsunami developments and management techniques. It is intended to be distributed within the scientific community and among the decision makers for tsunami risk reduction. The presented chapters have been thoroughly reviewed and accepted for publication. It presents advanced methods for tsunami measurement using Ocean-bottom pressure sensor, kinematic GPS buoy, satellite altimetry, Paleotsunami, Ionospheric sounding, early warning system, and scenario based numerical modeling. It continues to present case studies from the Northern Caribbean, Makran region and Tamil Nadu coast in India. Furthermore, classifying tsunamis into local, regional and global, their possible impact on the region and its immediate vicinity is highlighted. It also includes the effects of tsunami hazard on the coastal environment and infrastructure (structures, lifelines, water resources, bridges, dykes, etc.); and finally the need for emergency medical response preparedness and the prevention of psychological consequences of the affected survivors has been discussed.

InTech Europe
University Campus STeP Ri
Slavka Krautzeka 83/A
51000 Rijeka, Croatia
Phone: +385 (51) 770 447
Fax: +385 (51) 686 166
www.intechopen.com

InTech China
Unit 405, Office Block, Hotel Equatorial Shanghai
No.65, Yan An Road (West), Shanghai, 200040, China
中国上海市延安西路65号上海国际贵都大饭店办公楼405单元
Phone: +86-21-62489820
Fax: +86-21-62489821

IntechOpen